Oncogene (2002) 21, 890–898

www.nature.com/onc

Centrosome abnormalities, recurring deletions of chromosome 4, and genomic amplification of HER2/*neu* define mouse mammary gland adenocarcinomas induced by mutant HER2/*neu*

Cristina Montagna[1], Eran R Andrechek[2], Hesed Padilla-Nash[1], William J Muller[2] and Thomas Ried*[,1]

[1]*Genetics Branch, Center for Cancer Research, National Cancer Institute/NIH, Bethesda, Maryland, MD 20892, USA;* [2]*Department of Biology, Institute for Molecular Biology and Biotechnology, McMaster University, Hamilton, Ontario, ON L8S4K1, Canada*

The conditional expression of activated HER2/*neu* gene under its endogenous promoter in the mammary epithelium of the mouse results in accelerated lobular development and focal mammary tumors. Carcinogenesis, however, requires amplification and considerably increased expression levels of oncogenic *neu*. Deducing from the multiple genetic aberrations required for human breast cancer to develop, we hypothesized that in addition to the over-expression of an activated HER2/*neu*, secondary aberrations would occur. We have therefore conducted a genomic screen for chromosomal imbalances and translocations using comparative genomic hybridization and spectral karyotyping. The results reveal a moderate degree of chromosomal instability and micronuclei formation in short-term cultures established from primary tumors. Genomic instability appears to be linked to the amplification of functional centrosomes, a phenomenon that we frequently observed in other tumor types. Seventy per cent of the tumors revealed genomic amplification of HER2/*neu*, often in the form of double minute chromosomes, which correlated with recurring loss of mouse chromosome 4D-E, a region that is orthologous to distal human chromosome 1p. It is likely that this region contains putative tumor suppressor genes whose inactivation is required for tumor formation in this model of human breast cancer.
Oncogene (2002) **21,** 890–898. DOI: 10.1038/sj/onc/1205146

Keywords: HER2/*neu*; spectral karyotyping (SKY); breast cancer model; genomic instability; double minutes (DMs); centrosome

Introduction

Modeling human cancer in the mouse has become an increasingly valuable tool for understanding the genetic events responsible for tumor initiation and progression. Murine models can be used to monitor the effects of tissue specific elimination of tumor suppressor gene function and of the over-expression of cellular oncogenes. Numerous models for human breast cancer have been described (Hennighausen, 2000), many of which attempt to recapitulate the genetics of human breast cancer by over-expressing oncogenes known to be involved in the human disease. For instance, the forced expression of c-*myc*, HER2/*neu*, and cyclinD1, respectively, under the control of the mammary gland specific MMTV-promoter results in mammary gland adenocarcinomas (Muller *et al*., 1988; Stewart *et al*., 1984; Wang *et al*., 1994). Accordingly, the conditional, tissue specific depletion of BRCA1 function results in tumor formation (Xu *et al*., 1999a,b) and the impairment of *p53* and *RB1* function via expression of SV40 large T antigen under the control of the C3 promoter induces K-*ras* amplification and tumorigenesis (Liu *et al*., 1998). As in human cancers, it is likely that tumorigenesis in the mouse is promoted, or at least accompanied by, the acquisition of non-random chromosomal aneuploidies. For instance, human breast cancers frequently exhibit extra copies of chromosome 20, gains of chromosome arms 1q, 8q, and 17q, and losses that map to 8p and 17p (Ried *et al*., 1995; Tirkkonen *et al*., 1998). It would be intriguing to query whether this particular distribution of genomic imbalances is maintained in murine models of breast cancer despite the considerable shuffling of chromosomes during the course of evolution. Such comparative cytogenetic analyses, however, have been hampered by the intricacy of reliably karyotyping mouse chromosomes. We have therefore used spectral karyotyping (SKY) (Liyanage *et al*., 1996; Schröck *et al*., 1996b) and comparative genomic hybridization (CGH) (Kallioniemi *et al*., 1992; Weaver *et al*., 1999), two techniques that overcome these hurdles, to characterize chromosomal aberrations in a mouse model of human breast cancer induced by the expression of an activated

*Correspondence: T Ried, Genetics Branch, Center for Cancer Research, National Cancer Institute/NIH, Bldg. 9, Rm. 1N105, 9 Memorial Drive, Bethesda, MD 20892, USA;
E-mail: riedt@mail.nih.gov
Received 3 July 2001; revised 19 October 2001; accepted 31 October 2001

mutated HER2/*neu* under its endogenous promoter (Andrechek *et al*., 2000). As part of the family of epithelial growth factor receptors, the HER2/*neu* oncogene is amplified in about 25% of human breast cancers (Revillion *et al*., 1998). Genomic amplifications of the oncogenes HER2/*neu* and c-*myc* and potential deletions of the tumor suppressor genes *p53* and BRCA1 were assessed using fluorescence *in situ* hybridization. As a potential basis for the observed chromosomal aneuploidy we investigated centrosome integrity in these mammary cells using immunohistochemical visualization of γ-tubulin. We consider that such studies provide important baselines for the molecular analysis of murine tumors and contribute to the validation of mouse models for specific human cancers.

Results

The over-expression of an activated HER2/*neu* oncogene regulated via its physiological promoter results in the development of mammary gland adenocarcinomas in transgenic mice (Andrechek *et al*., 2000). Despite the fact that karyotype information could contribute to the validation of tumor models and provide entry points for the molecular cloning of cancer associated genes, data on chromosomal aberrations in murine carcinoma models remain sketchy.

In this study, we have applied molecular cytogenetic techniques, including SKY, CGH, and FISH with gene specific BAC clones to establish a comparative map of chromosomal aberrations in a series of 12 primary tumors induced by the expression of a constitutively activated HER2/*neu*. Karyotype analysis was performed on short-term cultures derived from primary tumors using SKY. An example of a SKY analysis is shown in Figure 1 for tumor #22. The most frequent chromosomal aberration was a deletion or monosomy of chromosome 4 (7 of 12 tumors). Except for the deleted chromosome 4, we could not detect recurring structural chromosomal aberrations, however, clonal numerical aberrations (chromosomal aneuploidies) were common. One tumor, #21, was normal both by SKY and CGH analysis. We cannot exclude that this is due to the preferential culture of fibroblasts or normal breast epithelial cells. With the exception of two tumors, in which we observed a diploid and tetraploid (#22) and triploid stem line (#19), the cells were predominantly diploid. Karyotypes for all of the tumors are summarized in Table 1 and can be retrieved from the SKY database at

Table 1 Summary of aberrations identified by SKY and CGH analysis for 12 HER2/*neu* primary tumors

Tumor	*SKY*	*CGH*
5	40, XX, Del(9?A1), +19, +50∼100dmin	−4, +11,Dp(11D)
6	40 XX	+6
15	38−40, XX, +2, Del(4D−E), Del(8?A1)+50∼100dmin	−13, Del(9F), Dp(11D), Del(14E)
15−17	37−54, XX,+X, Del(7?A1), −12, Del(14?A1), Del(18?A1), 50∼100dmin	nd
16	38−40, XX, Del(4D−E), +6+50∼100dmin Del(8?A1)	Dp(11D)
18	40−41, XX, Del(8?A1), Del(9?A1), Del(14?A1)	Del(9F), Dp(11D)
19	39−59, XX, +X, Del(8?A1), Del(9?A1)+11, −19, +50∼100dmin	Del(4E), Dp(11D), Del(14E)
20	40−41, XX, Del(9?A1)+15, +50∼100dmin	Del(9F), Dp(11E)
20/2	40−41, XX, +2, Del(4D−E), Del(9?A1)	−11
21	40 XX	−
22	40−87, XX, Del(4C−E), +5, Del(8?A1), Del(9?A1)+15, +19, 50∼100dmin	Dp(11D)
23	37−41 XX, +X, −4, Del(9?A1)+10, +50∼100dmin	Dp(11D)

Column 2 summarizes the karyotypes deduced by SKY. Column 3 shows the additional chromosomal gains and losses for each tumor as detected only by CGH

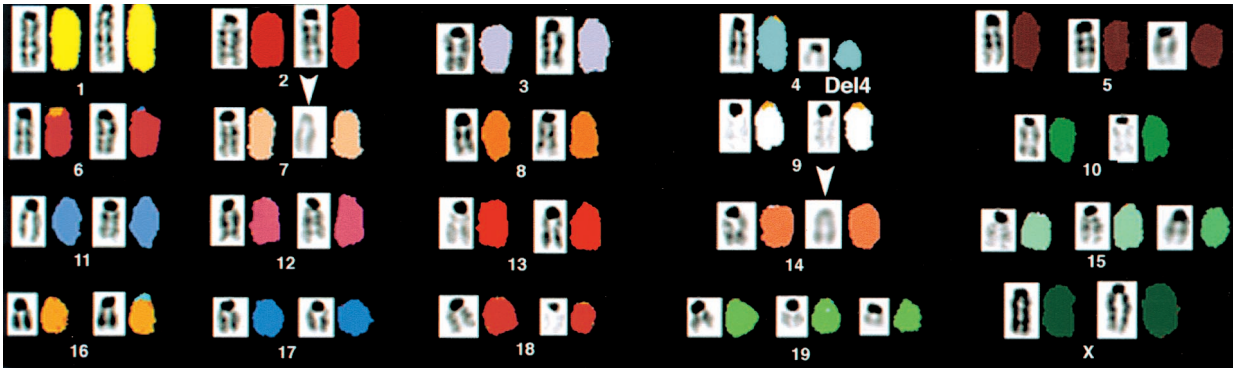

Figure 1 Spectral karyotyping (SKY) of mammary tumor cultures derived from MMTV-Cre Flox Neo NeuNT mice. A representative metaphase is given for #22. The karyotype is 43XX, Del(4D-E), Del(7A1), Del(14A1), +5, +15, +19 – Arrows denote the Del7 and Del14

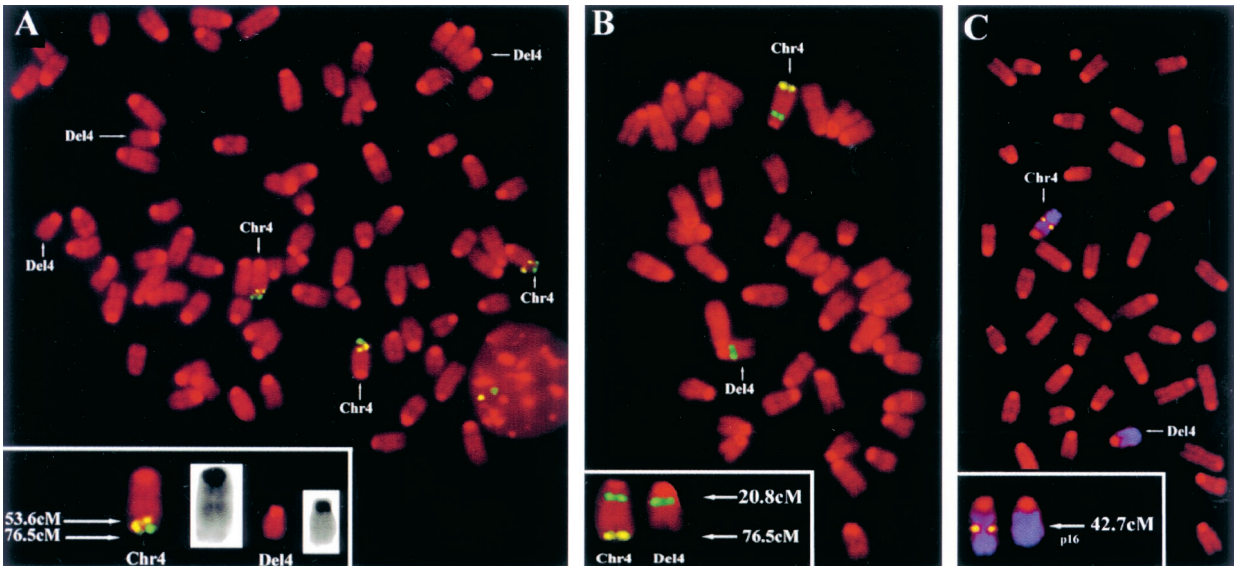

Figure 2 FISH experiment with four BAC clones specific for chromosome 4. (**a**) Shown is a triploid metaphase derived from tumor #22. The yellow signals reflect the hybridization of BAC clone 219G3, which maps at 53.6 cM. The green signals refer to clone 206N14, at the genetic locus 76.5 cM. The arrows in the box insert identify the signals in the normal alleles revealing two intact loci. The homologous chromosomes show no hybridization signals for either of the clones, suggesting a deletion of the region of at least 53.6–76.5 cM. (**b**) A diploid clone from the same tumor (#22) confirms the deletion of clone 204N14, however, clone 7J10 is retained. (**c**) In order to refine the breakpoint we used a clone for the tumor suppressor gene p16. The results demonstrate loss of one copy of this gene on the deleted chromosome 4

http://www.ncbi.nlm.nih.gov/sky/skyweb.cgi. As a means in establishing a quantitative measure for intra-tumor heterogeneity, we quantified the variation of chromosome numbers in individual cells. Gains or losses relative to the modal copy number of each chromosome in the tumor resulted in chromosomal instability indices ranging from 0.2–4. This is lower than that observed in aneuploid cell lines established from human carcinomas (MJ Difilippantonio, personal communication).

In order to define the deleted region of chromosome 4 with higher resolution, we used FISH with genetically mapped BAC clones to determine the smallest deleted interval. The hybridization patterns for tumor #22 are shown in Figure 2a–c. The results indicate BAC clones that map to 53.6 cM (D4Mit149) and 76.5 cM (D4Mit254) as well as a BAC clones for the tumor suppressor gene p16 (139P5 at 42.7 cM) are deleted on one allele, however, clone D4Mit229 (20.6 cM) is retained. The breakpoint is therefore proximal to 42.7 cM on the genetic map, which corresponds to chromosome band 4C3. This region of mouse chromosome 4, which was deleted in all but one tumor with chromosome 4 aberrations, is orthologous to human chromosome 1p32-1p36 and 9p.

Forty-eight per cent of the metaphases from 10 tumors analysed showed chromosomes that had acquired loss of the heterochromatic regions close to the centromere on band A1 (Figure 1). The chromosomes most commonly affected by the loss of the paracentromeric heterochromatic regionswere chromosomes 8 (five of 12 tumors), chromosome 9 (seven of 12 tumors), and less frequently chromosome 14 (two of 12 tumors), chromosome 7, 18 and X (one of 12 tumors, see also Table 1).

The analysis of human carcinomas using SKY and CGH has revealed that the majority of chromosomal aberrations result in genomic imbalances (Ghadimi *et al*., 1999), and that recurring copy number changes of particular chromosomes or chromosomal regions are a defining parameter of distinct human cancers (Ried *et al*., 1999). In order to establish comparative maps of genomic imbalances, the series of 12 murine mammary gland adenocarcinomas was analysed by CGH. The results are summarized in Figure 3 (see also the website http://www.ncbi.nlm.nih.gov/sky/skyweb.cgi for the CGH and SKY results). CGH confirmed the frequent loss of distal chromosome 4 as identified by SKY. High-level copy number increases that mapped to distal chromosome 11 were observed in six of 12 tumors, and low copy number increases in the same region were found in two additional tumors. In two cases (#20, #22) extra copies of chromosome 15 were detected. Both the c-*myc* oncogene and telomerase reverse transcriptase gene (hTRT) map to this chromosome. Less frequent copy number changes were observed on chromosome 2 (gained in #20/2 and #15) and 19 (gained in #5 and #22) and losses of the distal portion of chromosome 9 (#15, #18, #20). In total, we observed 34 copy number changes: divided by the number of cases, this translates to an average number of copy alterations (ANCA) of 2.8.

Eight of 12 tumors revealed metaphases containing extra-chromosomal DNA fragments whose shape was consistent with double minute chromosomes (DMs). The number of DMs ranged from 50 to 100 per cell (Figure 4b,c). DMs in solid tumors are frequently the

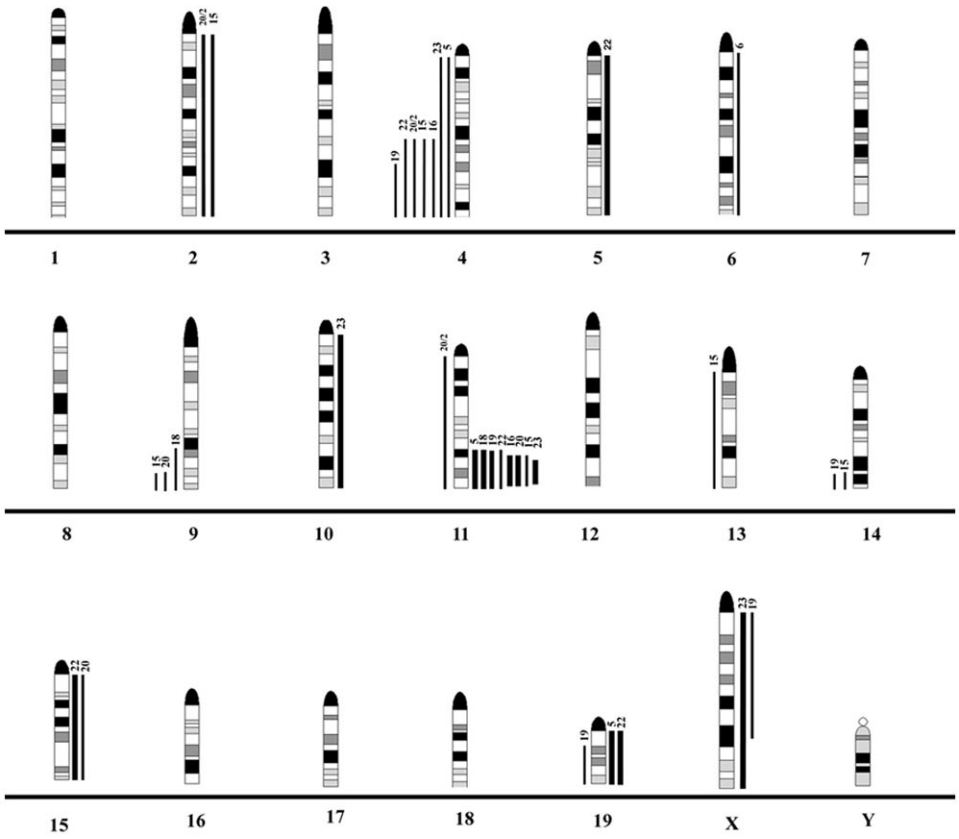

Figure 3 Summary of gains and losses in 12 mammary gland tumors based on CGH-analysis. The lines left to the ideogram denote genomic losses and the lines right to the chromosome ideogram gains of chromosomes. Bold lines indicate high-level copy number increases (amplifications). Note the frequent deletions on chromosome 4 and gains on chromosome 11. Individual case numbers are provided on top of the gain and loss bars

cytogenetic correlate of oncogene amplification (Alitalo *et al*., 1985). Since the amplicon identified by CGH mapped to the distal end of chromosome 11, we hypothesized that the HER2/*neu* gene, which maps to mouse chromosome 11 at 57 cM was the target for this gene amplification. FISH with a BAC clone specific for HER2/*neu* confirmed our hypothesis. Seven tumors contained greatly increased copy numbers of this oncogene located on the DMs (Figure 4b,c, Table 2). The genomic amplification detected by CGH is consistent with previous results using Southern-blot analysis with the exception of case #20, where CGH and FISH revealed greatly increased copy numbers for HER2/*neu*, however, amplification was not detected by Southern-blot analysis.

Genomic deletions frequently contribute to allelic loss and tumor suppressor gene inactivation in human cancers. We therefore investigated whether loss of the tumor suppressor genes *p53* and *brcal*, both involved in human breast cancers, were required for tumorigenesis in this mouse model. FISH analysis with a BAC clone for *brcal* clearly demonstrated that this tumor suppressor gene, which also maps to the distal end of chromosome 11 (Schröck *et al*., 1996a), was excluded from the amplicon and was present in two copies in diploid cells. We could also show that inactivation of *p53* (at least via chromosomal deletion) was not necessary for tumorigenesis because two copies were consistently observed in the diploid cells. The c-*myc* oncogene was not present in copy numbers higher than the ploidy of mouse chromosome 15. Examples of the FISH experiments are provided in Figure 4 and the results compiled in Table 2.

With one exception, all tumors revealed predominantly numerical chromosomal aberrations (Table 1). Such aberrations can be due to compromised chromosome segregation fidelity during mitotic cell division. The centrosome organizes the spindle apparatus prior to cell division and nucleates the proper assembly of microtubules whose attachment to the kinetochore at each chromosome is essential for correct segregation (Kellogg *et al*., 1994). We have previously shown that centrosome abnormalities occur exclusively in human colorectal carcinomas that are aneuploid, but not in their diploid, mismatch repair deficient counterparts (Ghadimi *et al*., 2000). We therefore wanted to investigate whether abnormalities and amplification of functional centrosomes could, at least partially, contribute to the observed chromosomal aneuploidy. The centrosome can be visualized using an antibody against γ-tubulin, a protein that is concentrated in the centrosome during all stages of the cell cycle. The

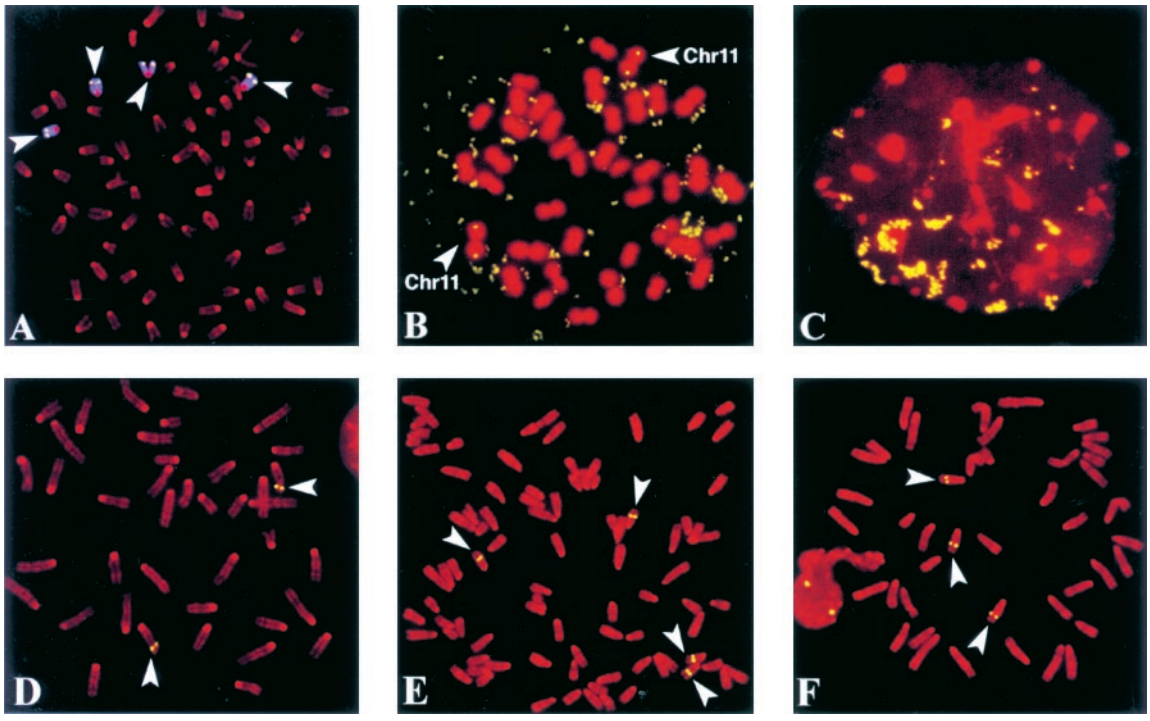

Figure 4 (**a**) Dual color FISH analyses of tumor #22 using a painting probe for chromosome 11 (blue) and a BAC clone specific for the HER2/*neu* oncogene (yellow). This tetraploid cell reveals four copies of an intact chromosome 11. No DMs were visible. (**b**) In contrast to the metaphase shown in **a**, the cell shown here reveals multiple DMs that labeled positively with the FISH probe for HER2/*neu* (yellow signals). Arrows denote the normal chromosome 11. (**c**) The interphase nuclei of tumor #22 show the amplification domains of HER2/*neu* after hybridization with the same FISH probe used in **a** and **b**. (**d**) FISH with a BAC clone for the tumor suppressor gene BRCA1 shows two signals on chromosome 11 in this diploid metaphase (tumor #22). (**e**) FISH with a BAC clone for the tumor suppressor gene *p53* did not reveal small interstitial deletions (yellow signals) in this tetraploid cell of tumor #22. (**f**) Tumor #22 reveals an extra copy of the c-*myc* oncogene on chromosome 15 (yellow). However, the copy number of the c-*myc* oncogene does not exceed the copy number of chromosome 15, hence no amplification

Table 2 Summary of FISH experiments

Tumor	*% cells + DM's*	*p53 deletion*	*BRCA1 deletion*	*c*-myc *amplif.*	*Centrosomes number*
5	100	nd	nd	nd	nd
6	nd	nd	nd	nd	nd
15	76	–	–	–	0–8
15–17	2	–	–	–	nd
16	96	–	–	–	nd
18	nd	nd	nd	nd	0–7
19	85	nd	nd	nd	1–2
20	50	–	–	–	0–10
20/2	nd	nd	nd	nd	nd
21	nd	nd	nd	nd	nd
22	81	–	–	–	nd
23	100	–	–	–	0–6

Column 2 indicates the per cent of cells containing double minute chromosomes for each sample. Columns 3, 4 and 5 show the results of FISH experiments with the BAC clones for the p53 and BRCA1 tumor suppressor genes and for the c-*myc* oncogene, respectively. Column 6 displays the enumeration of centrosome numbers using an antibody against γ-tubulin. nd, not determined

number of observed centrosomes in normal cells is cell cycle dependent as the centrosome is duplicated during S phase. Five tumor samples were analysed (#15, #18, #19, #20 and #23) and four of them revealed a significantly increased number of centrosomes. The average number per cell varied between 2.72 and 3.2, with up to 66% of the cells showing abnormal centrosome numbers. Besides the normal distribution of 1–2 centrosomes per cell (Figure 5a) we observed different patterns of centrosome abnormalities. In many instances, the centrosomes lined up similar to pearls on a string at the edge of the nucleus (Figure 5b). A second pattern displayed centrosomes located in the periphery of the cells and obviously detached from the nucleus (Figure 5c). The third pattern indicated centrosome replication in the absence of centrosome separation because clusters of centrosomes were observed near the nucleus (Figure 5d). Dual immunofluorescence using antibodies against α- and γ-tubulin was performed to assess whether supernumerary centrosomes were able to nucleate tubulin, form mitotic spindles and cause multipolar mitoses. The results shown in Figure 6 clearly demonstrate amplification of functional centrosomes. Evaluation of the nuclear DNA counterstain also showed the frequent occurrence of micronuclei. Micronuclei are indicative of chromosome breakage, increased formation of dicentric chromosomes, and lagging chromosomes due to errors in cell cycle timing (Müller *et al*., 1996). Twenty-five per cent of the cells were accompanied by micronuclei (as determined by propidium iodide

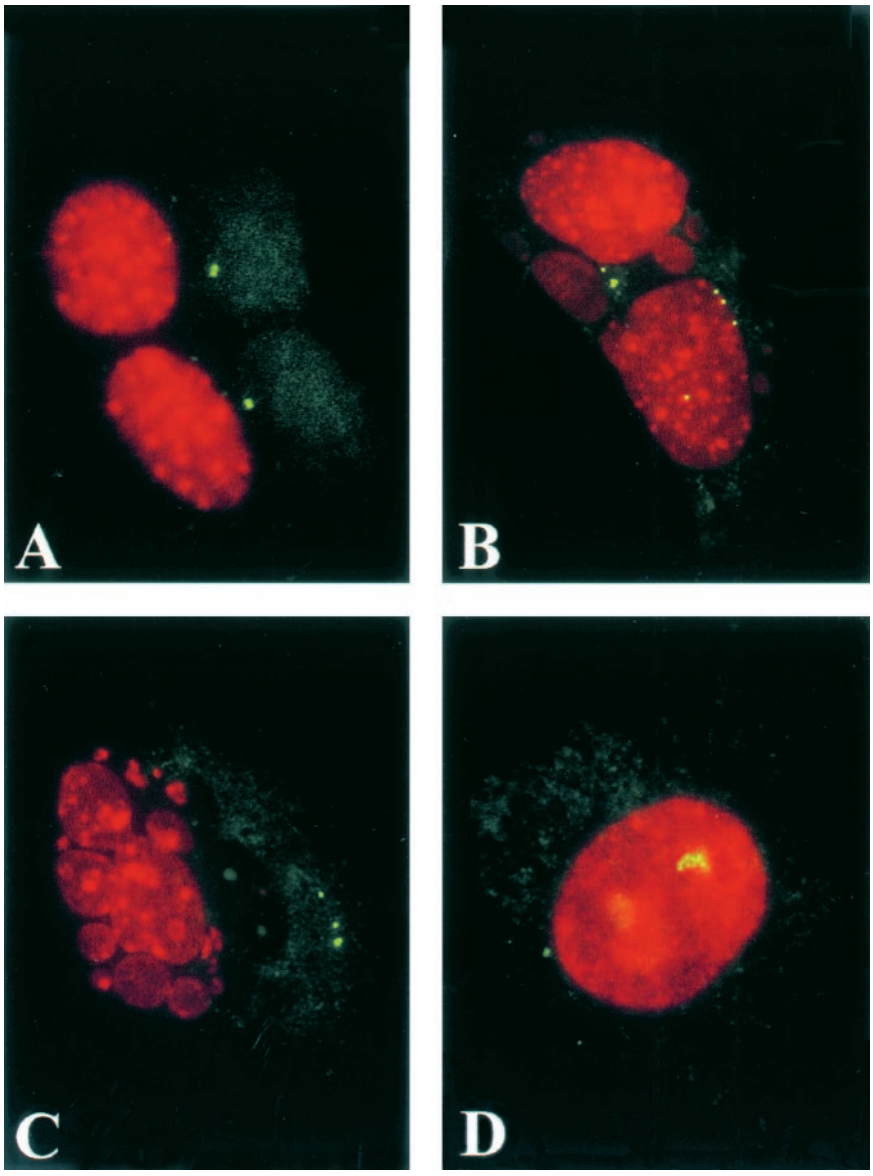

Figure 5 Immunocytochemistry with an antibody against γ-tubulin detects centrosomes. We observed four distinct patterns. (**a**) Normal centrosomes in an interphase nucleus. (**b**) Increased centrosome numbers that are aligned at the periphery of the nucleus. Note the presence of micronuclei. (**c**) Detached centrosomes in an apparently apoptotic cell. (**d**) Multiplied, but non separated centrosome in an interphase nucleus

staining), and approximately 60% revealed aberrant centrosome numbers. Micronuclei occurred only rarely in cells with normal centrosome numbers (7%) but were frequently found in cells with additional centrosomes (18%). However, we observed a significant number of cells with centrosome abnormalities in the absence of micronucleus formation (45% of all cells analysed).

Discussion

The acquisition of tumor specific patterns of chromosomal imbalances is a defining characteristic of cancers of epithelial origin. For instance, colorectal carcinomas almost invariably reveal copy number increases of chromosomes 7 and 13, and of chromosome arms 8q and 20q, while chromosome 18 is frequently lost (Ried *et al*., 1996). Also, the emergence of these chromosomal aneuploidies occurs in a more or less defined sequence of events. Trisomy of chromosome 7 is the earliest events that can already be observed in small polyps (Heim and Mitelman, 1995). Such a linear progression is less well established during breast carcinogenesis, however, it is clear that mammary tumors display a non-random involvement of certain chromosomes. Cytogenetic and molecular cytogenetic analyses have clearly shown that a gain of chromosome arm 1q, as well as gains of chromosome arms 8q and 17q accompanied by losses of the

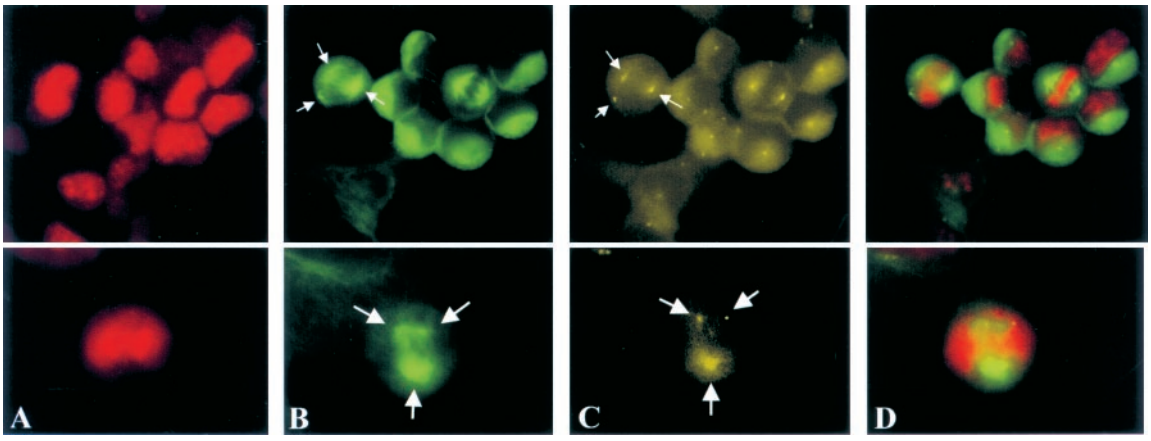

Figure 6 Dual-immunofluorescence with antibodies against α- and γ-tubulin to visualize centrosomes and spindle microtubules in tumor #22. (**a**) The DNA-counterstain. (**b**) α-tubulin staining in green. The arrows denote examples of multipolar mitotic cells. (**c**) Same cells as in **a** and **b** show the co-localization of γ-tubulin (arrows) with sites of α-tubulin aggregation indicating the nucleating capacity of supernumerary centrosomes. (**d**) Merged display of the individual images

respective short arms, are recurrently found in breast cancers (Heim and Mitelman, 1995). It is even possible to assign certain cytogenetic features to subgroups of breast cancers, that differ with respect to the nuclear DNA content, tumor size, lymph node status, and clinical course (Isola *et al*., 1995; Ried *et al*., 1995; Tirkkonen *et al*., 1998). Therefore, it appears that the acquisition and maintenance of a distinct pattern of genomic imbalances is a feature that is strongly selected for and maintained despite intra-tumor heterogeneity and chromosome instability. With this information in mind it is intriguing to determine (i) whether mouse models of different carcinomas share this characteristic pattern of chromosomal aneuploidy, and (ii) whether this pattern is dependent upon the mode of tumor induction. We have previously reported the molecular cytogenetic evaluation of mouse mammary gland adenocarcinomas induced by over-expression of the c-*myc* oncogene under the control of the MMTV-promoter (Weaver *et al*., 1999). Here we extend such comparative molecular cancer cytogenetics to the evaluation of tumors induced by the conditional expression of an activated HER2/*neu* gene under the transcriptional control of its endogenous promoter (Andrechek *et al*., 2000). During the course of mammalian chromosome evolution, human and mouse chromosomes have experienced a significant degree of reorganization (O'Brien *et al*., 1999). Comparison of chromosome aberration maps could therefore, with increased resolution, pinpoint genes whose involvement in tumorigenesis is required across species boundaries. Such a comparison would be particularly interesting for chromosomes that are found in a specific aberration pattern in human cancers, for instance as an isochromosome. Human chromosome 17 serves as such an example: sequences on chromosome arm 17p are frequently lost (with *p53* as the target), while chromosome 17q is often gained (including HER2/*neu* and as yet to be identified second oncogene on human chromosome 17q23), occasionally via isochromosome 17q formation. Since HER2/*neu* and *p53* both reside on the same arm of mouse chromosome 11 chromosome translocations or interstitial deletions would have to occur if deletions of *p53* and maintenance of HER2/*neu* are both required for tumorigenesis. Our molecular cytogenetic evaluation has shown that the tumors in this model system do not require the acquisition of the equivalent of an isochromosome 17q in human breast cancers. While the genomic amplification of HER2/*neu* is required for tumorigenesis, as illustrated by the presence of DMs, deletions of *p53* are not present.

CGH analysis clearly confirmed the genomic amplification of mouse chromosome 11C-D, the mapping position of the oncogene HER2/*neu* (11D). Of note, the same percentage of tumors revealed loss of distal mouse chromosome 4. The acquisition of HER2/*neu* amplification appeared to be linked to chromosome 4 deletions; only one tumor showed a gain of 11D that was not accompanied by the loss of parts or the entire homologue of chromosome 4. We had previously observed deletions of mouse chromosome 4 in MMTV-c-*myc* induced mammary gland adenocarcinomas (Weaver *et al*., 1999) and in conditional knockouts for the tumor suppressor gene BRCA1 (Weaver *et al*., submitted). These data therefore strongly suggest that a yet unidentified tumor suppressor gene resides at this chromosomal locus. This result is even more significant because distal mouse chromosome 4 is orthologous to human chromosome 1p. Human chromosome 1p has been shown in several reports to be subject to copy number loss in human breast cancers (Bieche *et al*., 1994). One potential candidate gene is p73, a member of the p53 gene family (Chen *et al*., 2001). Interestingly, in human neuroblastomas, genomic loss of chromosome 1p is associated with amplification of the n-*myc* oncogene, frequently in

the form of DMs (Bieche *et al*., 1994). One could hypothesize that the common and coordinate loss of chromosome band 4D and the emergence of DMs indicates that the function of a tumor suppressor gene in this region might extend to the suppression of gene amplification. The homology of distal mouse chromosome 4 also comprises region 9p21 in humans, which is the site of the p16INK4A and p19INK4d genes. These genes are involved in cellular senescence and immortalization and are therefore additional potential tumor suppressor candidate genes (Carnero *et al*., 2000).

Our data also suggest that neither copy number increases of the c-*myc* oncogene, nor deletions of the tumor suppressor genes *p53* or BRCA1, were required for tumorigenesis in this model. We can, however, not exclude the possibility of functional inactivation of either of these tumor suppressor genes by mechanisms different from chromosomal deletions. This is in contrast to tumors in conditional knockout mutants for BRCA1, in which both cytogenetic and Western-blot analyses suggest the frequent inactivation of *p53* (Weaver *et al*., submitted).

CGH analyses of human carcinomas have provided evidence that tumor staging and tumor aggressiveness correlate with the degree of genomic instability as measured by the average number of chromosomal aberrations (ANCA). For instance, diploid breast carcinomas display an ANCA index of 2.4–5, whereas aneuploid carcinomas, whose prognosis is much worse, show an ANCA of 6.8–12 (Ried *et al*., 1999). The ANCA index in the mouse models of human breast cancer that we have studied so far is in general similar to that observed in human carcinomas. In mammary gland adenocarcinomas induced by c-*myc* over-expression, the ANCA is 5.75, and in BRCA1-deficient aneuploid tumors 8.0. In the HER2/*neu* model only relatively few chromosomal aberrations were detected (ANCA = 2.8). It also appears that those tumor models that were induced by a strong oncogenic stimulus show fewer copy alterations than those induced by the tissue specific deletion of tumor suppressor genes. The lower ANCA value occurs even in the presence of considerable genetic heterogeneity from one tumor cell to another. It seems that a strong oncogenic stimulus overcomes the need for the acquisition and maintenance of numerous recurring chromosomal imbalances. We conclude that the sequential inactivation of multiple tumor suppressor genes, and the gain of function of several oncogenes by way of chromosomal abnormalities as seen in human breast carcinomas are reduced to the amplification of HER2/*neu* and loss of mouse chromosome 4D. One could extend this observation to the hypothesis that mouse tumor models induced by tumor suppressor gene deletion more closely reflect the nature of multi-step carcinogenesis that we observe in human epithelial cancers. Induction of tumors by oncogene over-expression, however, provides an excellent tool for analysing the particular pathways in which these genes are involved.

Materials and methods

Tissue culture and metaphase chromosome preparation

Mammary epithelial cell lines were derived from primary tumors of 12 different MMTV-Cre Flox Neo NeuNT knock-in mice (average latency 400 days). Tumor bearing animals (FVB 25%, CD1 25% and BALB/c 50%) were sacrificed and cell lines prepared from tumor tissue as previously described (Amundadottir *et al*., 1995; McCormack *et al*., 1998). Metaphase chromosomes were prepared following exposure to colcemid arrest (3–4 h, final concentration 100 μg/ml) and standard hypotonic treatment and fixation in methanol/acetic acid.

Molecular cytogenetic analyses

Spectral karyotyping was performed as described (Liyanage *et al*., 1996). Briefly, flow sorted normal mouse chromosomes were labeled with specific fluorochromes or fluorochrome combinations. After *in situ* hybridization images were acquired using an epifluorescence microscope (DMRXA, Leica, Wetzlar, Germany) connected to an imaging interferometer (SD200, Applied Spectral Imaging, Migdal HaEmek, Israel). Chromosomes were unambiguously identified using a spectral classification algorithm that results in the assignment of a separate classification color to all pixels with identical spectra (Garini *et al*., 1996). Chromosome aberrations were defined using the nomenclature rules from the International Committee on Standardized Genetic Nomenclature for Mice (Davisson, 1994). Six to 10 metaphases were analysed for each tumor. For CGH, DNA was prepared using high salt extraction and phenol purification and labeled by nick-translation using biotin-11-dUTP (Boehringer Mannheim, Indianapolis, IN, USA). Genomic DNA from strain-matched mice was prepared and labeled with digoxigenin-12-dUTP (Boehringer Mannheim). Hybridization was performed on karyotypically normal metaphase chromosomes (FVB strain) using an excess of mouse Cotl-DNA (Gibco-BRL, Gaithersburg, MD, USA). The biotin-labeled sequences were visualized with avidin-FITC (Vector Laboratories, Burlingame, CA, USA) and the digoxigenin labeled sequences were detected with a mouse derived antibody against digoxigenin followed by a secondary rhodamine conjugated anti mouse antibody (Sigma-Aldrich, Milwaukee, WI, USA). Quantitative fluorescence imaging and CGH analysis was performed using Leica Q-CGH software (Leica Imaging Systems, Cambridge, UK). BAC clones (Research Genetics, Huntsville, AL, USA) containing locus specific sequences for the oncogenes HER2/*neu* and c-*myc* and the tumor suppressor genes BRCA1 and *p53* and four BAC clones isolated from the RCPI23 genomic library containing the markers D4Mit149 (clone name 215G3), D4Mit254 (204N14), D4Mit229 (7J10), and 139P5 (specific for the p16 tumor suppressor gene) were used in this study. FISH probes were labeled with biotin or digoxigenin by nick translation and hybridized to chromosome preparations derived from the primary tumors. After over night hybridization at 37°C, the slides were detected with FITC-conjugated avidin (Vector Laboratories, Burlingame, CA, USA) and TRITC-conjugated anti-digoxigenin antibodies, respectively (Sigma-Aldrich, St. Louis, MO, USA).

Immunohistochemistry

Cells were cultured on Falcon chamber slides (Thomas Scientific, Swedesboro, NJ, USA), washed in PBS, and fixed

with MetOH (0°C) for 10 min and washed again in PBS. Incubation with a monoclonal anti γ-tubulin antibody (Sigma, St. Louis, MO, USA) diluted 1 : 1000 in 3% goat serum/PBS was performed overnight at 37°C. The antibody complexes were detected with TRITC-conjugated goat anti-rabbit IgG (Sigma, St. Louis, MO, USA) and counterstained with DAPI. When dual immunofluorescence experiments were performed, we used a polyclonal anti γ-tubulin antibody (Sigma) and a monoclonal anti α-tubulin antibody (Sigma). Gray level images were acquired using a CCD camera (CH250, Photometrics, Tucson, AZ, USA) mounted on a Leica DMRBE epifluorescence microscope, and pseudo-colored using Leica Q-Fish software. Further details for all Materials and methods can be found at http://www.riedlab.nci.nih.gov/.

Acknowledgments
The authors would like to thank Michael J Difilippantonio, Kerstin Heselmeyer-Haddad, Joseph Cheng and Buddy Chen for critically reading and editing the manuscript. ER Andrechek was supported by the US Army Scholarship #DAMD17-99-1-9285.

References

Alitalo K, Saksela K, Winqvist R, Alitalo R, Keski-Oja J, Laiho M, Ilvonen M, Knuutila S and de la Chapelle A. (1985). *Lancet,* **2,** 1035 – 1039.

Amundadottir LT, Johnson MD, Merlino G, Smith GH and Dickson RB. (1995). *Cell Growth Differ.,* **6,** 737 – 748.

Andrechek ER, Hardy WR, Siegel PM, Rudnicki MA, Cardiff RD and Muller WJ. (2000). *Proc. Natl. Acad. Sci. USA,* **97,** 3444 – 3449.

Bieche I, Champeme MH and Lidereau R. (1994). *Cancer Res.,* **54,** 4274 – 4276.

Carnero A, Hudson JD, Price CM and Beach DH. (2000). *Nat. Cell Biol.,* **2,** 148 – 155.

Chen X, Zheng Y, Zhu J, Jiang J and Wang J. (2001). *Oncogene,* **20,** 769 – 774.

Davisson MT. (1994). *Gene,* **147,** 157 – 160.

Garini Y, Macville M, du Manoir S, Buckwald RA, Lavi M, Katzir N, Wine D, Bar-Am I, Schröck E, Cabib D and Ried T. (1996). *Bioimaging,* **4,** 65 – 72.

Ghadimi BM, Sackett DL, Difilippantonio MJ, Schröck E, Neumann T, Jauho A, Auer G and Ried T. (2000). *Genes Chrom. Cancer,* **27,** 183 – 190.

Ghadimi BM, Schröck E, Walker RL, Wangsa D, Jauho A, Meltzer PS and Ried T. (1999). *Am. J. Pathol.,* **154,** 525 – 536.

Heim S and Mitelman F. (1995). *Cancer Cytogenetics*. Wiley-Liss.

Hennighausen L. (ed). (2000). *Oncogene (Rev.),* **19,** 966 – 967.

Isola JJ, Kallioniemi OP, Chu LW, Fuqua SA, Hilsenbeck SG, Osborne CK and Waldman FM. (1995). *Am. J. Pathol.,* **147,** 905 – 911.

Kallioniemi A, Kallioniemi O-P, Sudar D, Rutovitz D, Gray JW, Waldman F and Pinkel D. (1992). *Science,* **258,** 818 – 821.

Kellogg DR, Moritz M and Alberts BM. (1994). *Annu. Rev. Biochem.,* **63,** 639 – 674.

Liu ML, Von Lintig FC, Liyanage M, Shibata MA, Jorcyk CL, Ried T, Boss GR and Green JE. (1998). *Oncogene,* **17,** 2403 – 2411.

Liyanage M, Coleman A, du Manoir S, Veldman T, McCormack S, Dickson RB, Barlow C, Wynshaw-Boris A, Janz S, Wienberg J, Ferguson-Smith MA, Schröck E and Ried T. (1996). *Nat. Genet.,* **14,** 312 – 315.

McCormack SJ, Weaver Z, Deming S, Natarajan G, Torri J, Johnson MD, Liyanage M, Ried T and Dickson RB. (1998). *Oncogene,* **16,** 2755 – 2766.

Muller WJ, Sinn E, Pattengale PK, Wallace R and Leder P. (1988). *Cell,* **54,** 105 – 115.

Müller WU, Nusse M, Miller BM, Slavotinek A, Viaggi S and Streffer C. (1996). *Mutat. Res.,* **366,** 163 – 169.

O'Brien SJ, Menotti-Raymond M, Murphy WJ, Nash WG, Wienberg J, Stanyon R, Copeland NG, Jenkins NA, Womack JE and Marshall Graves JA. (1999). *Science,* **286,** 458 – 462, 479 – 481.

Revillion F, Bonneterre J and Peyrat JP. (1998). *Eur. J. Cancer,* **34,** 791 – 808.

Ried T, Just KE, Holtgreve-Grez H, du Manoir S, Speicher MR, Schröck E, Latham C, Blegen H, Zetterberg A, Cremer T and Aver G. (1995). *Cancer Res.,* **55,** 5415 – 5423.

Ried T, Knutzen R, Steinbeck R, Blegen H, Schröck E, Heselmeyer K, du Manoir S and Auer G. (1996). *Genes Chrom. Cancer,* **15,** 234 – 245.

Ried T, Heselmeyer-Haddad K, Blegen H, Schröck E and Auer G. (1999). *Genes Chrom. Cancer,* **25,** 195 – 204.

Schröck E, Badger P, Larson D, Erdos M, Wynshaw-Boris A, Ried T and Brody L. (1996a). *Hum. Genet.,* **97,** 256 – 259.

Schröck E, du Manoir S, Veldman T, Schoell B, Wienberg J, Ferguson-Smith MA, Ning Y, Ledbetter DH, Bar-Am I, Soenksen D, Garini Y and Ried T. (1996b). *Science,* **273,** 494 – 497.

Stewart TA, Pattengale PK and Leder P. (1984). *Cell,* **38,** 627 – 637.

Tirkkonen M, Tanner M, Karhu R, Kallioniemi A, Isola J and Kallioniemi OP. (1998). *Genes Chrom. Cancer,* **21,** 177 – 184.

Wang TC, Cardiff RD, Zukerberg L, Lees E, Arnold A and Schmidt EV. (1994). *Nature,* **369,** 669 – 671.

Weaver ZA, McCormack SJ, Liyanage M, du Manoir S, Coleman A, Schröck E, Dickson RB and Ried T. (1999). *Genes Chrom. Cancer,* **25,** 251 – 260.

Xu X, Wagner KU, Larson D, Weaver Z, Li C, Ried T, Henninghausen L, Wynshaw-Boris A and Deng CX. (1999a). *Nat. Genet.,* **22,** 37 – 43.

Xu X, Weaver Z, Linke SP, Li C, Gotay J, Wang XW, Harris CC, Ried T and Deng CX. (1999b). *Mol. Cell,* **3,** 389 – 395.